

Vortex shedding patterns, their competition, and chaos in flow past inline oscillating rectangular cylinders

Srikanth T., Harish N. Dixit, Rao Tatavarti, and Rama Govindarajan

Citation: *Physics of Fluids* (1994-present) **23**, 073603 (2011); doi: 10.1063/1.3610389

View online: <http://dx.doi.org/10.1063/1.3610389>

View Table of Contents: <http://scitation.aip.org/content/aip/journal/pof2/23/7?ver=pdfcov>

Published by the [AIP Publishing](#)

Articles you may be interested in

[Shallow flow past a cavity: Coupling with a standing gravity wave](#)

Phys. Fluids **24**, 104103 (2012); 10.1063/1.4761829

[Flow past a normal flat plate undergoing inline oscillations](#)

Phys. Fluids **24**, 093603 (2012); 10.1063/1.4749803

[Pulsatile flow past an oscillating cylinder](#)

Phys. Fluids **23**, 041903 (2011); 10.1063/1.3576186

[Vortex shedding from a step-cylinder in spanwise sheared flow](#)

Phys. Fluids **23**, 035109 (2011); 10.1063/1.3560385

[Dynamics of vortex lock-on in a perturbed cylinder wake](#)

Phys. Fluids **18**, 074103 (2006); 10.1063/1.2221350



Vortex shedding patterns, their competition, and chaos in flow past inline oscillating rectangular cylinders

Srikanth T.,¹ Harish N. Dixit,^{1,a)} Rao Tataavarti,² and Rama Govindarajan^{1,b)}

¹Engineering Mechanics Unit, Jawaharlal Nehru Centre for Advanced Scientific Research, Jakkur, Bangalore 560064, India

²Department of Civil Engineering, Gayatri Vidya Parishad College of Engineering, Madhurawada, Visakhapatnam 530048, India

(Received 10 December 2010; accepted 9 June 2011; published online 27 July 2011)

The flow past inline oscillating rectangular cylinders is studied numerically at a Reynolds number representative of two-dimensional flow. A symmetric mode, known as S-II, consisting of a pair of oppositely signed vortices on each side, observed recently in experiments, is obtained computationally. A new symmetric mode, named here as S-III, is also found. At low oscillation amplitudes, the vortex shedding pattern transitions from antisymmetric to symmetric smoothly via a regime of intermediate phase. At higher amplitudes, this intermediate regime is chaotic. The finding of chaos extends and complements the recent work of Perdikaris *et al.* [Phys. Fluids **21**(10), 101705 (2009)]. Moreover, it shows that the chaos results from a competition between antisymmetric and symmetric shedding modes. For smaller amplitude oscillations, rectangular cylinders rather than square are seen to facilitate these observations. A global, and very reliable, measure is used to establish the existence of chaos. © 2011 American Institute of Physics. [doi:10.1063/1.3610389]

I. INTRODUCTION

Vortex shedding from bluff bodies is an extensively studied problem. The preferred mode of vortex shedding, in the uniform flow past a fixed body, is antisymmetric. On the other hand, the mode of shedding in the case of an inline oscillating cylinder in a uniform flow can be antisymmetric, symmetric, or chaotic depending on the forcing frequency and amplitude. Thus, for a body oscillating inline in a uniform external flow, as the frequency of oscillation is increased with all other parameters remaining fixed, we may expect a transition from antisymmetric to symmetric shedding. Both kinds of shedding have been observed.¹⁻⁵ Second, it has been seen experimentally that there is more than one kind of symmetric shedding.⁶ Our objective here is to improve our understanding of the frequency response of the system, in terms of the spatial arrangements of vortices and the transitions therein. Studies on such flows have found application in predicting the loading on offshore structures.⁷ Also, this is a simple example of the flow due to an accelerating body. The prediction of flow patterns in its wake can be important in various contexts, such as in the tracking of underwater bodies.

Griffin and Ramberg⁸ were among the first to study vortex shedding from an inline oscillating circular cylinder in a freestream. They found that the vortex shedding frequency locks on to the frequency of cylinder oscillation for $1.2 \leq f_e/f_o \leq 2.5$, where f_e is the frequency of cylinder oscillation and f_o would have been the frequency of vortex shedding if the cylinder were held stationary. The subscripts e and o have been chosen to stand for “excitation” and

“original,” respectively. Both primary lock-on, where the shedding frequency $f_s = f_e$, and subharmonic lock-on, with $f_s = f_e/2$ were observed. Ongoren and Rockwell² carried out experiments with a circular cylinder oscillating at an angle α with a uniform freestream. Outside the lock-on regime, competition between symmetric and antisymmetric modes in the form of switching of modes in a single experiment was observed. In some recent experiments, Konstantinidis and Balabani⁵ too noted the symmetric mode mentioned above, where all vortices shed from the top wall were of one sign, while those shed from the bottom wall were of the opposite sign. This pattern is called the S-I mode of shedding. In another experimental study, on a circular cylinder, Xu *et al.*⁶ discovered a new mode of symmetric shedding, which they named S-II. Two vortices of opposite sense were shed from each side (top and bottom) during each cycle. This mode was observed for high frequencies and amplitudes. There was considerable reverse flow during a part of the cycle, which aided in the formation of opposite signed vortices on a given side of the cylinder. Very few numerical studies have reported the symmetric S-I shedding, Zhou and Graham’s⁴ being one. To our knowledge, the S-II mode has not been found numerically before.

Besides systematic shedding, we could have chaotic shedding. Chaos in flow around an inline oscillating circular cylinder (or equivalently, in oscillating flow past a fixed cylinder) was reported by Vittori and Blondeaux⁹ and Perdikaris *et al.*¹⁰ The former study had no mean flow and showed that the route to chaos is quasiperiodic, and the latter study attributed chaos to mode competition. However, no evidence of mode competition was provided. One goal of the present study is to present direct evidence of competition between antisymmetric and symmetric shedding and the resulting chaos. Ciliberto and Gollub^{11,12} showed that competition

^{a)}Present address: Mathematics Department, University of British Columbia, Vancouver V6T 1Z2, Canada.

^{b)}Electronic mail: rama@jncasr.ac.in.

between different modes in parametrically forced surface waves can result in chaos. Their study also revealed the existence of chaotic “windows.” They remarked that this could be a common cause of chaos in systems in which different spatial structures can exist. The present flow is shown to be one example.

In a circular or square cylinder, the behaviour of each row of shed vortices can be clouded by interaction with the opposite row. For this reason, we study the flow past rectangular cylinders of various aspect ratios. To our knowledge, there have been no previous studies on vortex shedding from inline oscillating rectangular cylinders. We show the existence of symmetric S-I and S-II modes, and a new S-III mode, besides the Couder-Basdevant mode. Along with a discussion for the occurrence of the new S-III mode, we then discuss a physical mechanism for the enhancement of S-II shedding from rectangular cylinders. We show that the transition from antisymmetric to symmetric shedding, as f_e is increased, for lower oscillation amplitudes occurs via periodic flows of different phase. At higher oscillation amplitudes, we find windows of chaos between the regimes where shedding modes are antisymmetric and symmetric.

II. PROBLEM FORMULATION

The numerical procedure described in Dixit and Babu¹³ was employed after making suitable changes. Flow solutions are obtained by solving the Lattice-Boltzmann equation

$$f_i(X_k + e_{ik}, t + 1) = f_i(X_k, t) + \frac{1}{\tau}(f_i^{eq}(X_k, t) - f_i(X_k, t)). \quad (1)$$

As in the usual nomenclature, $f_i(X_k, t)$ and $f_i^{eq}(X_k, t)$ are the nonequilibrium and equilibrium distribution functions in i th direction and τ is the time between two successive collisions. Thus, the density $\rho = \sum_i f_i$ and the momentum vector is $\rho u_k = \sum_i f_i e_{ik}$. No-slip on walls is imposed by employing the bounce-back scheme.

It is straightforward to show that in the absence of rotation of the cylinder, the vorticity and continuity equations in a cylinder-fixed frame are the same as those in the lab-fixed frame. In the cylinder-fixed coordinate system, we have an oscillating inlet flow,¹⁴ $u_x = U_\infty + A\Omega \sin \Omega t$, A is the amplitude of the displacement of the body, Ω ($\equiv 2\pi f_e$) is the frequency of oscillation, and u_x and u_y are the streamwise and transverse components of fluid velocity, respectively. The other boundary conditions are $\partial u_x / \partial x = \partial u_y / \partial x = 0$ at the outlet, $u_x = u_y = 0$ on the cylinder, and $u_x = U_\infty + A\Omega \sin \Omega t$, $u_y = 0$ at the top and bottom surfaces. The characteristic length in this study is taken to be the height D of the body, and the characteristic velocity is U_∞ , so the Reynolds number is defined as $Re \equiv U_\infty D / \nu$ and the Strouhal number as $St \equiv f_s D / U_\infty$, f_s being the shedding frequency of the vortices.

Figure 1(a) shows a part of the domain used for the simulations. The size of the domain is $75D \times 75D$ with nonuniform grids of up to a million grid points, whose arrangement is shown in Figure 1(b). The values for the domain size and number of grid points were arrived at after doing a grid and domain independence study. The grid resolution is fine, with

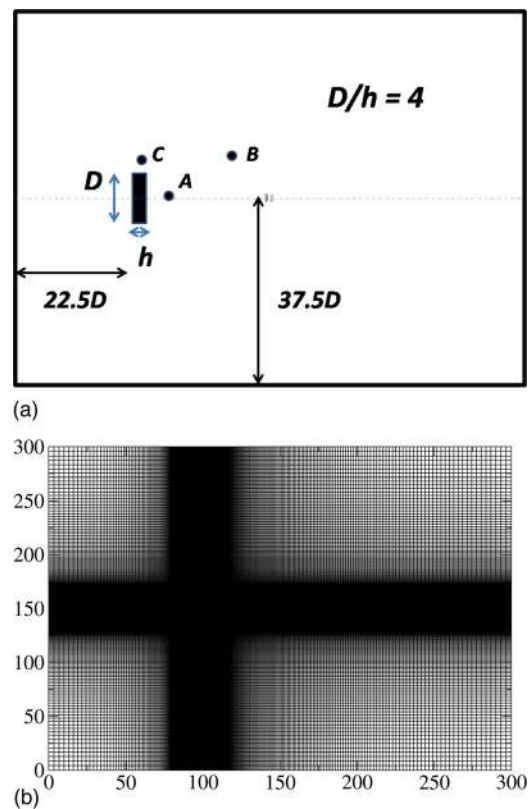


FIG. 1. (Color online) (a) Schematic of the domain used in the simulations. Time signals are stored at the monitor points A, B, and C, located at $(2h, 0)$, (h, D) and $(2.25D, 0.5D)$, respectively, (not to scale). (b) The grid used.

80 points per unit length on the body surface. The reason for the use of a large domain is twofold: to minimize the effects of outlet boundary conditions on the wake and to ensure that the symmetric modes are insensitive to the lateral and longitudinal extents of the domain. All simulations in this study were carried out at $Re = 200$.

The numerical approach was validated as follows. Strouhal numbers obtained from flow past a fixed square cylinder were found to be in good agreement for a range of Reynolds numbers with those from Okajima’s experiments¹⁵ and Ansumali *et al.*’s numerical simulations.¹⁶ With an oscillating square cylinder, the dominant frequencies in the spectrum for the wall normal velocity u_y at a typical location obtained from our simulations agree well with the spectrum for the lift coefficient obtained by Minewitsch *et al.*¹⁴ for this geometry. This is shown in Fig. 2. Next, as done in Ref. 14, the frequency ratio was fixed at $f_e/f_o = 1.6$, and A/D varied from 0.15 to 0.4 in steps of 0.05. In excellent agreement with Ref. 14, the lock-on window between $0.15 \leq A/D \leq 0.4$, where $f_s = 0.5f_e$ is reproduced.

For $Re = 200$, $A/D = 0.175$, and $f_e/f_o = 2$ in the square cylinder case, the vorticity field qualitatively matches with one of the experimental results of Couder and Basdevant.¹⁷ This mode, shown in Figure 3(a), consists of two rows: one with binary vortices and the other with single vortices. We are able to obtain the S-II mode of vortex shedding behind a square cylinder, Figure 3(b), for $Re = 200$, $A/D = 0.5$, and $f_e/f_o = 1.73$. Xu *et al.*⁶ were the first to report the S-II mode of shedding experimentally in the case of a circular cylinder.

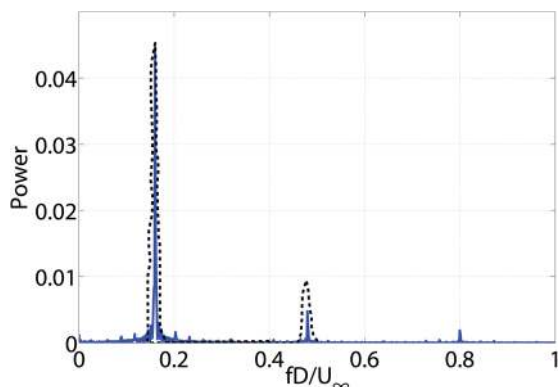


FIG. 2. (Color online) Comparison between the spectra obtained from Minewitsch *et al.* (Ref. 14) (dashed line) and the present code (solid line) for $Re=200$, $A/D=0.25$, and $f_e=0.32U_\infty/D$. The present spectrum is obtained from the time signal of u_y at monitor point A in Fig. 1(a). The power spectrum of Minewitsch *et al.* is that of their lift coefficient and has been arbitrarily scaled.

The amplitude ratio and frequency were the same in their experiment as the values used here, but their Reynolds number was 500. To the best of our knowledge, the S-II and Couder-Basdevant modes have not been seen computationally before.

III. RESULTS

A. Modes of vortex shedding

When the oscillation frequency f_e is very small, the flow is not too different from that past a fixed cylinder, except that the Reynolds number now is slowly varying. One expects, and finds, a slightly modified Karman street behind the body in this case. The same is true when the amplitude of oscillation

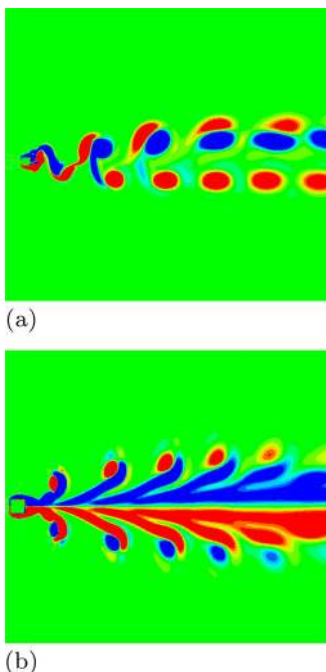


FIG. 3. (Color online) Qualitative comparison of shedding modes for the square cylinder. Vorticity fields are shown. (a) $f_e/f_o=2$ and $A/D=0.175$. This mode is similar to the one obtained by Couder and Basdevant. (Ref. 17) (b) $f_e/f_o=1.73$ and $A/D=0.5$. This is S-II mode of shedding, similar to that seen in the experiment of Xu *et al.* (Ref. 6).

tion A/D is small, since the oncoming flow merely sees a slightly modified body on an average. To observe competition between symmetric and antisymmetric shedding, one needs an effective oscillation Reynolds number $Re_o = (\Omega A)D/\nu$ which is not negligible compared to that of the incoming flow. Although we carried out many simulations to ensure that our results are general, we present only a few typical ones. The shedding pattern changes as the excitation frequency f_e is increased from $0.5f_o$, half the natural shedding frequency of a stationary cylinder, to five times this value, some examples are shown in Figure 4. A rectangular cylinder

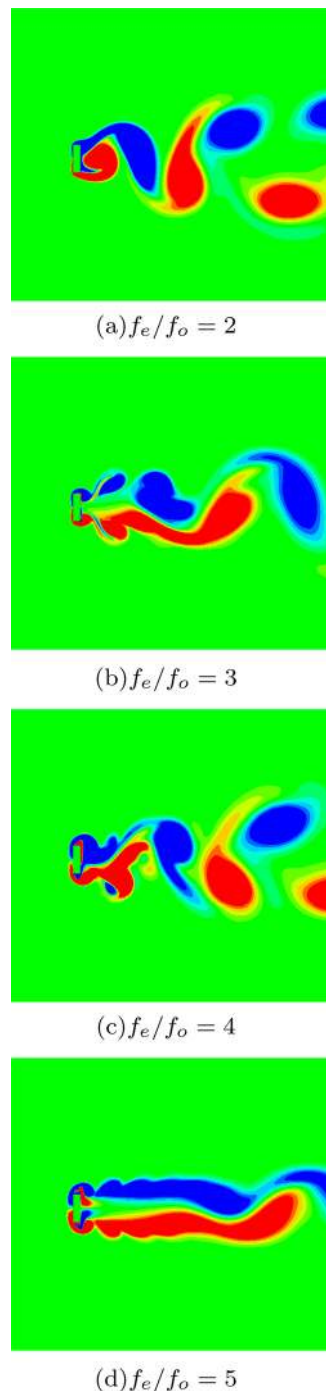


FIG. 4. (Color online) Vorticity fields at a typical time for $A/D=0.1$ at various excitation frequencies for a cylinder of aspect ratio 4. (a) $f_e/f_o=2$, (b) $f_e/f_o=3$, (c) $f_e/f_o=4$, and (d) $f_e/f_o=5$.

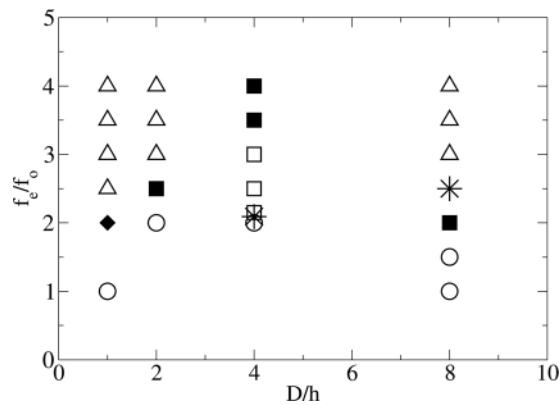


FIG. 5. Flow patterns in the wake of an incline oscillating rectangular cylinder at $Re=200$ and $A/D=0.175$. Circles: antisymmetric shedding, squares: symmetric shedding. The solid squares indicate the S-II mode, the open squares stand for the S-I mode, while the patterned square indicates an S-III shedding. Triangles: mixed mode, where the shedding is symmetric but the vortices arrange themselves into an antisymmetric pattern downstream. Stars: chaotic flow, single solid diamond: the Couder-Basdevant mode.

of aspect ratio 4 is used here and A/D is fixed at 0.1. At low f_e , the shedding is antisymmetric and goes to symmetric shedding as f_e increases. At $f_e/f_o = 5$, we have the symmetric S-I mode, with all the top vortices being of one sign and all the bottom of the opposite sign. At moderate f_e/f_o , the shedding is neither symmetric nor antisymmetric, but the upper and lower vortices are shed with a phase between 0 and π (or π and 2π). The flow, however, is still periodic. In some cases, vortex merger on each side of the cylinder is promoted, and the pattern downstream becomes antisymmetric. At small f_e , the shedding frequency f_s is close to f_o . However, as f_e/f_o is increased beyond 2, f_s decreases before locking on to a subharmonic of f_e , and then starts increasing proportionately with f_e , such that $f_s/f_e = 0.25$ for $3 \leq f_e/f_o \leq 4$. Beyond this range, f_s steadily decreases with further increase in f_e . The lock-on is similar to those seen on circular cylinders.⁵ Note that at these high frequencies, shedding occurs on a given surface once every four complete oscillations, rather than once in every other oscillation.

Next, choosing $A/D = 0.175$, we summarise in Figure 5 the patterns of vortex shedding observed on cylinders with aspect ratio $D/h = 1, 2, 4$, and 8. This higher oscillation amplitude will be seen to contrast with the lower A/D discussed above, in particular in the transition from an antisymmetric pattern of shedding to a symmetric. In the case of a square cross section, one would have to go to high amplitudes of oscillation to observe symmetric shedding. We benefit by the use of rectangular geometries, where a small oscillation amplitude is sufficient to observe different modes of shedding in the typical range of frequencies we use. The symmetric modes obtained may be classified into three types, S-I to S-III. As mentioned earlier, the first two have been observed in experiments before, but on circular cylinders.^{2,6} The letter S signifies a symmetric pattern, while the number denotes how many pairs of shed vortices may be associated with one time period of the flow. Thus, the cylinder sheds one vortex of each sign both at the top and the bottom in an S-II mode. At higher oscillation frequencies, the flow displays what we term as a mixed mode.

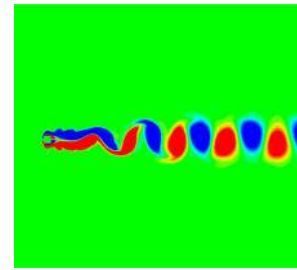


FIG. 6. (Color online) Mixed mode in the case of square cylinder, $f_e/f_o = 4$, $A/D = 0.175$.

To discuss the mixed mode, shown in Figure 6, we choose a square geometry. Such a pattern has also been seen by Konstantinidis and Balabani.⁵ The shedding off the cylinder is actually symmetric, but some distance downstream, the shed vortices arrange themselves in an antisymmetric pattern, much like a Karman street, but with a larger spacing and a correspondingly lower Strouhal number of 0.92 times that of a fixed square cylinder at this Reynolds number. The oscillating square cylinder together with the symmetric portion of its wake corresponds roughly to a stationary body with an effective D/h less than 1. In fact, the Strouhal number of the downstream portion of this figure is the same as that of a body whose aspect ratio is 0.67. In taller geometries, the mixed mode is actually encouraged to occur by merger events of vortices of one sign, some of which are evident in Figures 4(b) and 4(c). The downstream behaviour again becomes antisymmetric. With all other parameters held constant, and reducing h alone, i.e., using a taller rectangular cylinder rather than a square, we would reduce the relative size of the boundary layer and therefore the strength of the shed vortex. The pressure oscillations, which normally promote antisymmetric shedding, are correspondingly reduced, and so the symmetric pattern should persist further downstream for a given oscillation frequency. This is indeed manifested (not shown).

Returning to our discussion on the aspect ratio of 4, the wake pattern changes from a Karman street, followed by a chaotic pattern, through S-III and then S-II, followed by S-I with increase in the frequency of oscillation. The S-III mode, shown in Figure 7(a), is simply the S-II mode with an extra pair of vortices appearing close to the centreline. It is classified separately since it appears on the other side of chaos in the transition from antisymmetric shedding. A sample of S-II shedding on this cylinder is shown in Figure 7(b).

The dominant frequency for $f_e/f_o = 2$ is $f_s = f_o$ (Figure 8). This is indicative of subharmonic lock-on,^{1,8} while the shedding is locked on to the oscillation of the cylinder in the S-III mode.

B. Mechanism for S-II and S-III modes

Figure 9 shows the time signal of the vorticity ω at the monitor point C. In the absence of a mean flow, it is easy to visualise the alternate shedding of oppositely signed vortices when the cylinder is moving to and fro. The mean flow advects both vortices downstream. This S-II mode of

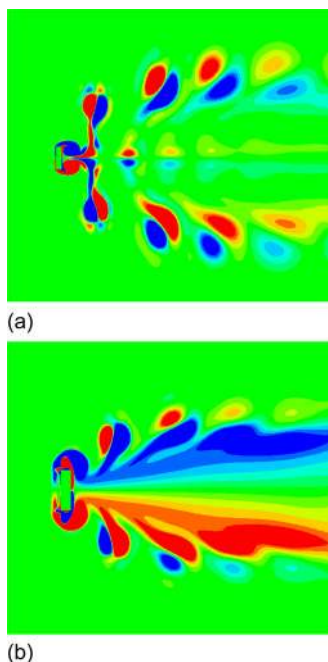


FIG. 7. (Color online) Two of the modes of shedding at $A/D=0.175$ on a body of aspect ratio 4. (a) The S-III mode at $f_e/f_o=2.15$. Three pairs of binary vortices are shed. (b) The S-II mode at $f_e/f_o=4$. In this mode, two binary vortices are shed during each time period.

shedding is aided by the “ground effect.” The primary vortices accelerate the fluid in the wake region towards the cylinder, and due to the larger area available on a rectangle rather than a square at the lee surface, significant vorticity

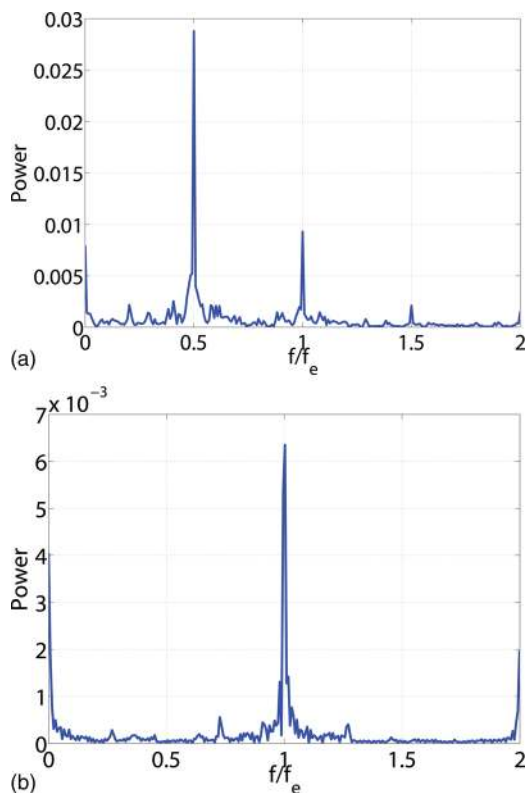


FIG. 8. (Color online) Power spectra at the monitor point A for $D/h=4$ and $A/D=0.175$. (a) Subharmonic shedding at $f_e/f_o=2$. (b) The shedding is harmonic (symmetric) for $f_e/f_o=2.15$.

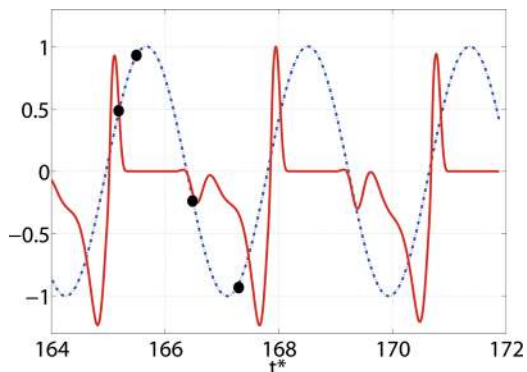


FIG. 9. (Color online) Phase information for the S-II mode for $D/h=8$. Solid line: the vorticity ω at monitor point B. Dashed line: inlet velocity U_{inlet} . Here, $f_e/f_o=2$ and $A/D=0.175$. The circles indicate the phases at which the vorticity field is shown in Figures 10(a)–10(d).

of opposite sign is generated. This effect is similar to the one studied by Carnevale *et al.*¹⁸ on a different problem.

This ground effect is clearly visible on a rectangle of aspect ratio 8. The circles in Figure 9 indicate the time instants at which vorticity field is plotted in Figures 10(a)–10(d). In Figure 10(a), the cylinder is moving upstream. The primary vortices are seen to form just behind the top and bottom surfaces of the cylinder. Vorticity is continuously supplied to them in the usual manner by the boundary layers. As these primary vortices grow, they accelerate the fluid in the wake region leading to the formation of boundary layers, Figure 10(b), on the lee side of the cylinder of oppositely signed vorticity with respect to the primary vortices. Now, when the cylinder moves downstream, there is a local reverse flow near the cylinder. This causes shape changes in both vortices. The secondary vortices continue to grow and cut off supply to the primary vortices as can be seen in Figs. 10(c) and 10(d). This cycle repeats. In the experiments of Xu *et al.*,⁶ there was considerable overall reverse flow which aided the formation of opposite signed vortices on the surface of a circular cylinder. Here, aided by the ground effect, we obtain the S-II mode even without reverse flow at the inlet.

The formation of the S-III mode involves the ground effect too. However, the vorticity field is more complex than in the S-II mode during the intermediate stages. Since the frequency is slightly lower in this case, there is time for the secondary vortex to get stretched due to the action of both the vortex being generated on the surface and the vortex which has just been dislodged from the cylinder. This leads to the pinching off of the secondary vortex at a point close to the primary vortex and thus the generation of an extra pair of vortices which move along the centerline. Figures 11(a) and 11(b) show two phases of this process.

An obvious difference between our geometries and a circular cylinder, even when the cylinders are fixed, is that the separation points are fixed at the sharp corners in our case, but are Reynolds number dependent in the circular cylinder. No other qualitative difference is evident in this range of Reynolds numbers. The basic difference between a square and rectangular geometry is that the ground effect is more

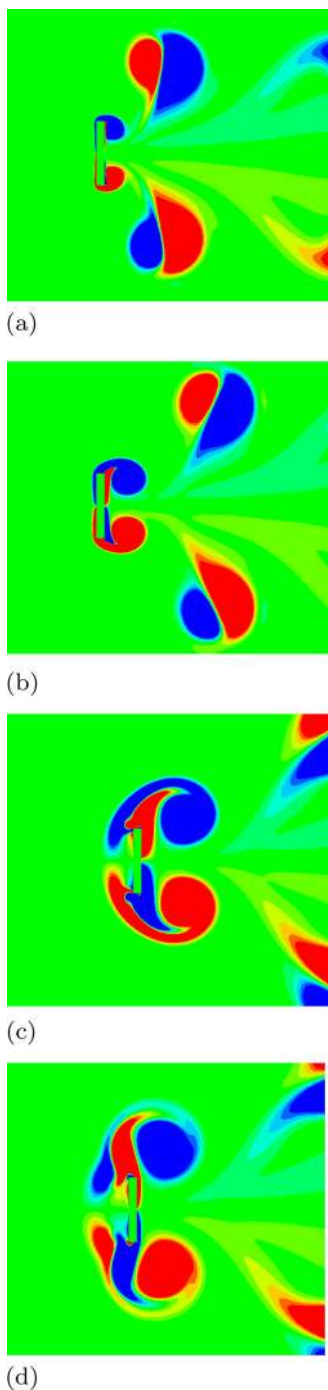


FIG. 10. (Color online) The S-II mode of vortex shedding; $D/h=8$, $f_e/f_o=2$, and $A/D=0.175$. Time has been non-dimensionalized using the convective time-scale, D/U_∞ . (a) Attached primary vortices are growing. (b) Vorticity is generated on the lee side. (c) Close to the cylinder, the flow is from right to left. The primary vortices are pushed apart and the secondary vortices are “stretched.” (d) The secondary vortices cut off the supply to primary.

pronounced in the latter, when the two are oscillating. The larger surface available on the rear side relative to the horizontal surfaces on a rectangular cross-section means that boundary layer effects from the rear can compete with those from the top and bottom. Other things held fixed, a rectangular geometry can thus provide a range of possibilities not all accessible to a square.

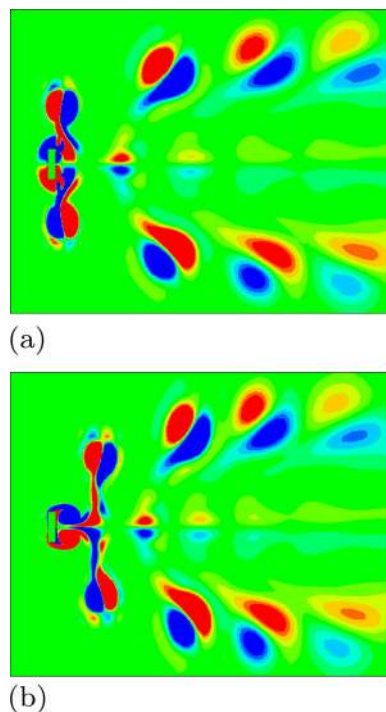


FIG. 11. (Color online) The S-III mode of vortex shedding; $D/h=4$, $f_e/f_o=2.15$, and $A/D=0.175$. In both figures, the cylinder is moving towards the left (upstream). (a) The stretching of secondary vortices has begun, and they are about to be dislodged from the cylinder by the next pair of primary vortices. (b) The central part of the secondary vortices has thinned, creating a pinch off of an extra pair vortices which then move along the centreline.

C. Mode competition and chaos

Perdikaris *et al.*¹⁰ reported chaotic flow in the wake of a circular cylinder placed in a uniform flow at one particular amplitude of inline oscillation. In their simulations, the cylinder was forced at the corresponding Strouhal frequency of the fixed cylinder. At about the same time, without being aware of that work, we had obtained chaotic flow using square and rectangular cylinders. We thus confirm their appealing finding. Further, while they surmised that a competition between antisymmetric and symmetric shedding was causing chaos, they did not have direct evidence for this. In particular, their lift coefficients and spectra indicate antisymmetric shedding under all non-chaotic conditions, so they do not have mode competition between antisymmetric and symmetric modes. For the values of nondimensional numbers used, the use of a rectangular cross-section makes it easy to obtain symmetric shedding, so we are able to demonstrate that the shedding is antisymmetric at f_e less than for the chaotic flow and symmetric for f_e greater than this value, which is a direct demonstration of mode competition in the sense of Ciliberto and Gollub.^{11,12}

In Figure 13(c), typical delay plots, for u_y at $f_e/f_o=2$ and 2.085, are shown. The axes on the delay plots represent $V_1 = u_y(t + \tau)$ and $V_2 = u_y(t - \tau)$ at a suitably chosen location and delay time τ . In Figure 12(a), the paths in phase space are closed, which indicates periodicity. The noise in the computations gives rise to a patch rather than a single path, as

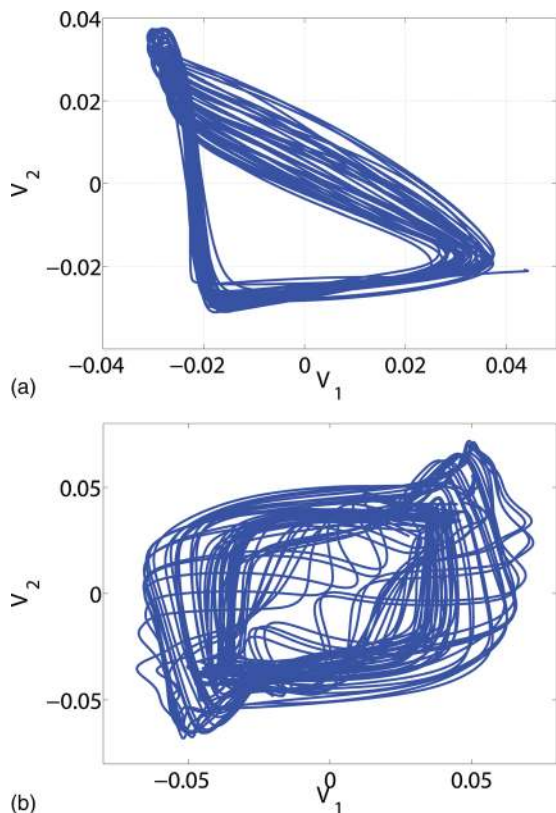


FIG. 12. (Color online) Delay plots for $D/h=4$, $f_e/f_o=2$, and 2.085. The oscillation amplitude $A/D=0.175$. The monitor point is behind the cylinder at $(0.5D, 0.35D)$. The delay plot (a) consists of closed curves, indicating periodicity, whereas (b) is characteristic of an aperiodic time signal. The delay time used is $\tau^* \equiv \tau D/U_\infty=2$.

often happens in these computations. In spite of this noise, this figure may easily be contrasted with Figure 12(b), which is indicative of a chaotic flow. The chaotic window is easily visualised in Figure 13, with the antisymmetric mode, locked on to $0.5f_e$, and the S-III mode, locked on to f_e , on either side of the narrow window of chaotic flow in between.

Thus far, we have obtained qualitative indications of the chaotic window. To confirm that the flow is indeed chaotic, we use a global measure $S(\Delta t)$ defined as

$$S = \sum_i \sum_j [\omega(x_i, y_j, t_o + \Delta t) - \omega(x_i, y_j, t_o)]^2 \Delta x \Delta y. \quad (2)$$

Being an integrated quantity over the entire domain, S is a reliable measure of chaos. For a periodic system of period T , $S(T)=0$. Moreover, for any Δt , we should have $S(\Delta t+T) = S(\Delta t)$. For $f_e/f_o=2$ and $f_e/f_o=2.15$, both these properties are seen in Figure 14. In particular, a sharp dip in S for $\Delta t = nT$ for any integer n is visible. On the other hand, for $f_e/f_o=2.085$, S remains at a high value, characterising a chaotic system.

A different behaviour is seen at $D/h=8$. The vortex shedding mode changes from S-II to the mixed mode with S-I shedding when f_e/f_o is varied from 2 to 3.5. Figure 16 shows that the flow for $f_e/f_o=2$ is periodic. However, the flow is chaotic for $f_e/f_o=2.5$, as evidenced by the spectrum in Figure 15(a). Also the arrangement of vortices at a given time is in no particular pattern, as seen in Figure 15(b). The

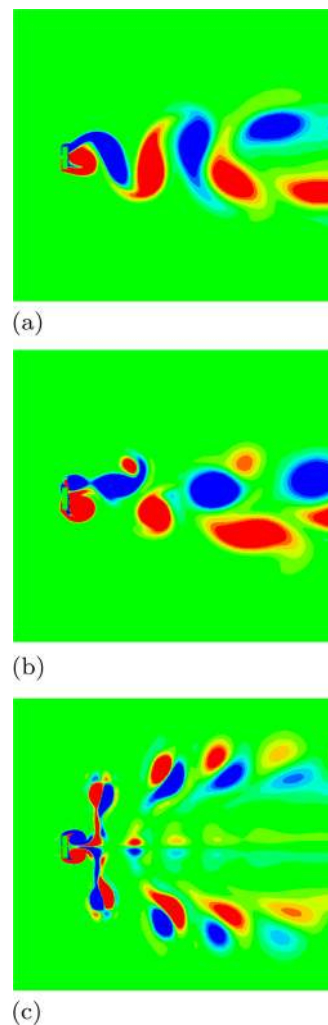


FIG. 13. (Color online) Chaotic window for $D/h=4$. (a) $f_e/f_o=2$, the shedding here is antisymmetric. (b) $f_e/f_o=2.085$, the shedding is chaotic. (c) $f_e/f_o=2.15$, S-III mode of symmetric shedding.

contrast in terms of the S is demonstrated in Figure 16. A smaller region is chosen to improve the contrast. The variation of S for $f_e/f_o=2$ is seen to be periodic, whereas for $f_e/f_o=2.5$ it is not.

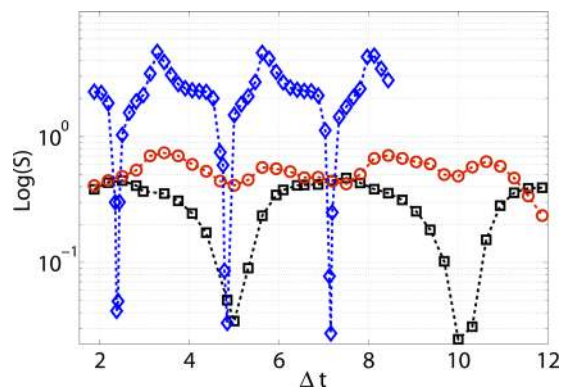


FIG. 14. (Color online) $D/h=4$. Variation of S with Δt for different cases. Squares: $f_e/f_o=2$, circles: $f_e/f_o=2.085$, and diamonds: $f_e/f_o=2.15$. The first and third curves exhibit periodicity and have sharp dips at $\Delta t = nT$ for any integer n , whereas the second curve is aperiodic.

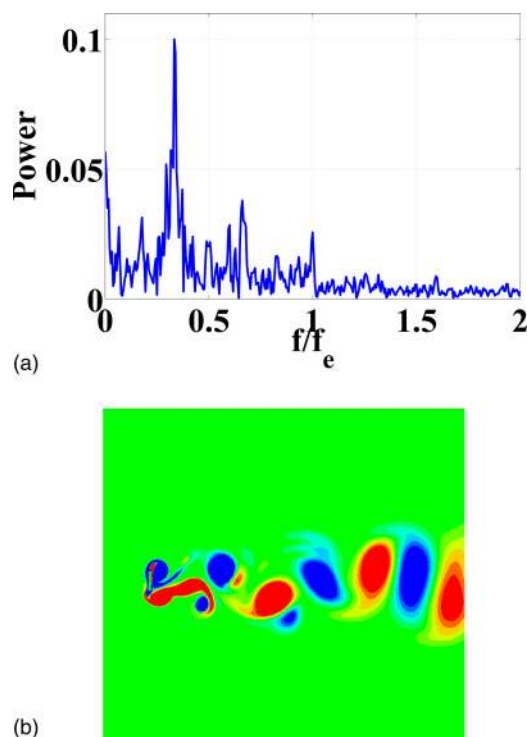


FIG. 15. (Color online) $D/h=8$, $f_e/f_o=2.5$, and $A/D=0.175$. (a) The spectrum is broadband, and (b) the arrangement of vortices is unordered, showing that the flow is chaotic.

IV. CONCLUSIONS

To summarise, we have studied two-dimensional flow past inline oscillating cylinders of rectangular cross-section at a relatively low Reynolds number. The S-II mode of shedding is obtained computationally for the first time to our knowledge. A variant symmetric mode, named here as S-III is also observed. The ground effect is pronounced in a rectangular cylinder making it possible to observe these modes at lower oscillation amplitudes than on a square. The type of shedding changes as the frequency of cylinder oscillation is increased, all other parameters held constant. At lower oscillation amplitudes, the frequency regime in between the anti-

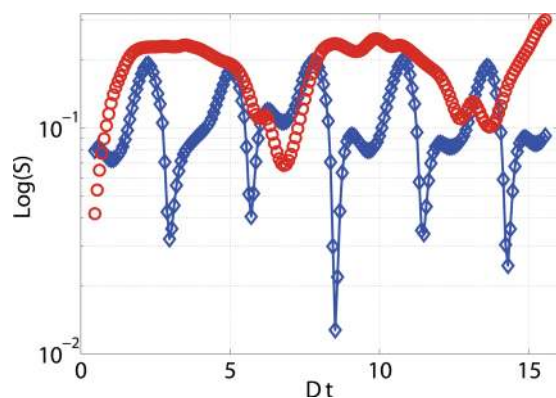


FIG. 16. (Color online) $D/h=8$. Variation of S with Δt in a region $x/D=2.5-8.75$. Diamonds: $f_e/f_o=2$, and is repetitive indicating periodicity. Circles: $f_e/f_o=2.5$, and shows the aperiodic nature of the vorticity field in that region.

symmetric and symmetric modes consists of a periodic flow where the shedding is neither symmetric nor antisymmetric, but a constant phase is maintained between shedding on the upper and lower surfaces. At higher oscillation frequencies, the flow in this intermediate frequency regime is chaotic. More than one window of chaos may exist in the frequency range. Since these windows always lie between regimes of antisymmetric and symmetric shedding, the chaos is due to mode competition in the sense of Ciliberto and Gollub.¹¹ The shedding frequency in the periodic regimes on either side of the chaotic window are locked-on to two different submultiples of the excitation frequency.

The use of a rectangular cylinder rather than a square one has made several of the above observations possible. A global, and therefore reliable, measure has been used to ascertain the existence of chaos. It is hoped that the present results will motivate experiments with rectangular oscillating cylinders. The work also presents natural extensions to flow past accelerating bodies.

ACKNOWLEDGMENTS

The authors would like to thank Professor Ram Ramaswamy and Dr. Santosh Ansumali for helpful discussions on chaos and the Lattice-Boltzmann method, respectively. The Naval Physical and Oceanic Labs, Kochi, is gratefully acknowledged for a grant which enabled this work to begin.

- ¹C. Barbi, D. P. Favier, C. A. Maresca, and D. P. Telionis, "Vortex shedding and lock-on of a circular cylinder in oscillatory flow," *J. Fluid Mech.* **170**, 527 (1986).
- ²A. Ongoren and D. Rockwell, "Flow structure from an oscillating cylinder Part 2. Mode competition in the near wake," *J. Fluid Mech.* **191**, 225 (1988).
- ³E. Detemple-Laake and H. Eckelmann, "Phenomenology of Karman vortex streets in oscillatory flow," *Exp. Fluids* **7**, 217 (1989).
- ⁴C. Y. Zhou and J. M. R. Graham, "A numerical study of cylinders in waves and currents," *J. Fluids Struct.* **14**, 403 (2000).
- ⁵E. Konstantinidis and S. Balabani, "Symmetric vortex shedding in the near wake of a circular cylinder due to streamwise perturbations," *J. Fluids Struct.* **23**, 1047 (2007).
- ⁶S. J. Xu, Y. Zhou, and M. H. Wang, "A symmetric binary-vortex street behind a longitudinally oscillating cylinder," *J. Fluid Mech.* **556**, 27 (2006).
- ⁷C. H. K. Williamson, "Vortex dynamics in the cylinder wake," *Annu. Rev. Fluid Mech.* **28**, 477 (1996).
- ⁸O. N. Griffin and S. E. Ramberg, "The vortex street wakes of vibrating cylinders," *J. Fluid Mech.* **66**, 553 (1974).
- ⁹G. Vittori and P. Blondeaux, "Quasiperiodicity and phase locking route to chaos in 2-D oscillatory flow around a circular cylinder," *Phys. Fluids A* **5**(8), 1866 (1993).
- ¹⁰P. G. Perdikaris, L. Kaiaksis, and G. S. Triantafyllou, "Chaos in a cylinder wake due to forcing at the Strouhal frequency," *Phys. Fluids* **21**, 101705 (2009).
- ¹¹S. Ciliberto and J. P. Gollub, "Pattern competition leads to chaos," *Phys. Rev. Lett.* **52**, 922 (1984).
- ¹²S. Ciliberto and J. P. Gollub, "Chaotic mode competition in parametrically forced surface waves," *J. Fluid Mech.* **158**, 381 (1985).
- ¹³H. N. Dixit and V. Babu, "Simulation of high Rayleigh number natural convection in a square cavity using the lattice Boltzmann method," *Int. J. Heat Mass Transfer* **49**, 727 (2006).
- ¹⁴S. Mineswitsch, R. Franke, and W. Rodi, "Numerical investigation of laminar vortex-shedding flow past a square cylinder oscillating in line with the mean flow," *J. Fluids Struct.* **8**, 787 (1994).
- ¹⁵A. Okajima, "Strouhal numbers of rectangular cylinders," *J. Fluid Mech.* **123**, 379 (1982).

- ¹⁶S. Ansumali, S. S. Chikatamarla, C. E. Frouzakis and K. Boulouchos, "Entropic Lattice Boltzmann Simulation of the Flow Past Square Cylinder," *Int. J. Mod. Phys. C* **15**(3), 435 (2004).
- ¹⁷Y. Couder and C. Basdevant, "Experimental and numerical study of vortex couples in two-dimensional flows," *J. Fluid Mech.* **173**, 225 (1986).
- ¹⁸G. F. Carnevale, O. U. Velasco Fuentes, and P. Orlandi, "Inviscid dipole-vortex rebound from a wall or coast," *J. Fluid Mech.* **351**, 75 (1997).
- ¹⁹M. Provansal, C. Mathis, and L. Boyer, "Benard-von Karman instability: Transient and forced regimes," *J. Fluid Mech.* **182**, 1 (1987).
- ²⁰K. R. Sreenivasan, P. J. Strykowski, and D. J. Olinger, "Hopf bifurcation, Landau equation and vortex shedding behind circular cylinders," in *Proceedings of the Forum on unsteady flow separation*, Cincinnati, OH, June 14–17 (A88-14141 03-34) (American Society of Mechanical Engineers, New York, 1987), p. 1–13.
- ²¹J. H. Gerrard, "The mechanics of the formation region of vortices behind bluff bodies," *J. Fluid Mech.* **25**, 401 (1966).
- ²²L. D. Landau and E. M. Lifshitz, "Course of theoretical physics," in *Fluid Mechanics* (Butterworth-Heinemann, New Delhi, 2005), Vol. 6.